



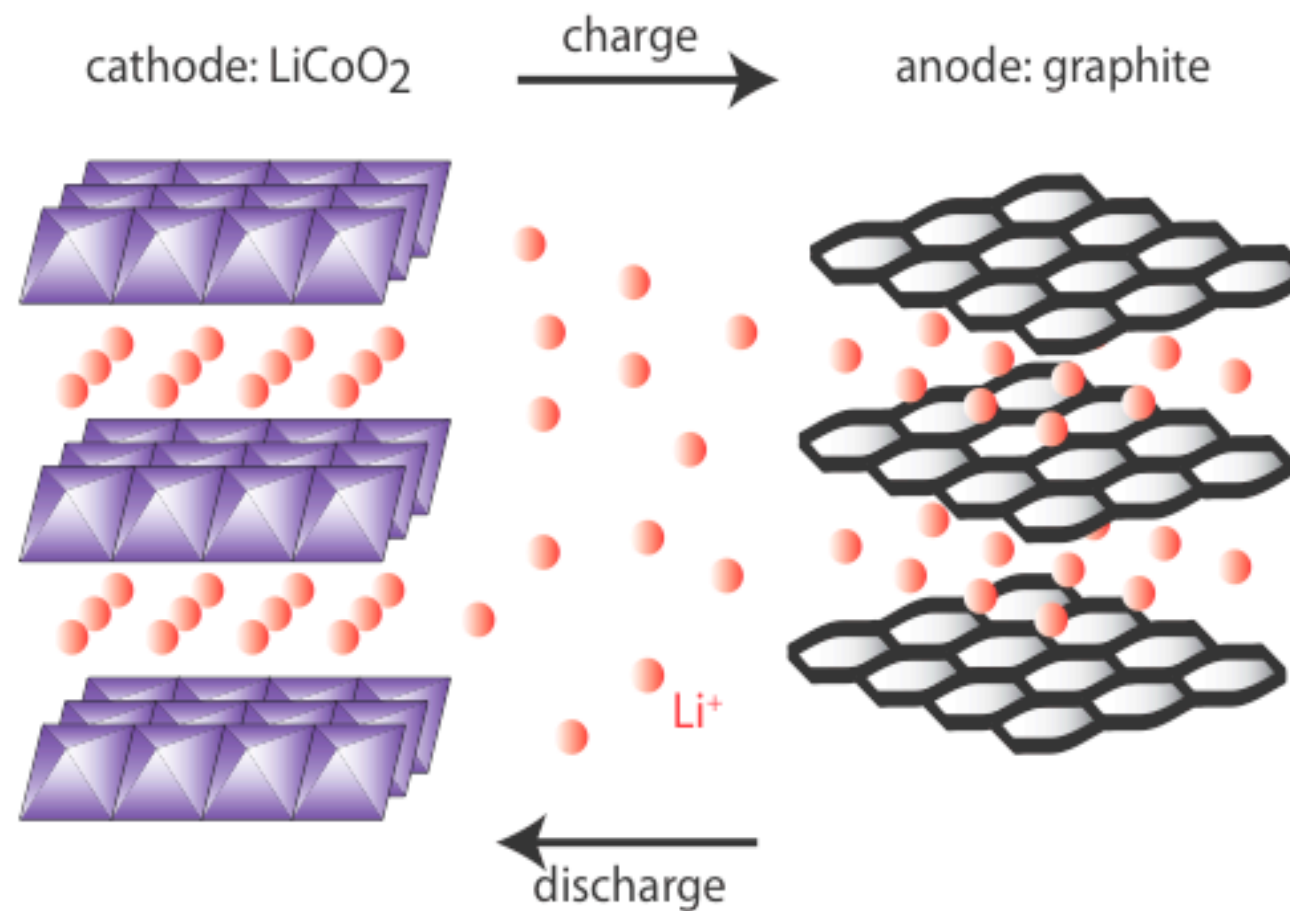
Solid-state NMR studies of lithium superionic conductors

Jeremy Titman,
School of Chemistry, University of Nottingham

Lithium batteries

Commercial rechargeable lithium batteries

- ★ The cell voltage corresponds to the difference in the Li^+ insertion potential in the two electrode materials
- ★ Charge / discharge cycles involve Li^+ ions shuttling between the electrodes



NMR studies of lithium superionic conductors

Structure

- ★ the electrochemistry of the charging process
- ★ the role of defects in ionic conduction
- ★ changes in structure on extended cycling

Dynamics

- ★ timescales, activation energies and mechanism of the underlying ionic diffusion
- ★ correlation effects, motional heterogeneity

Comparison of ^6Li and ^7Li NMR

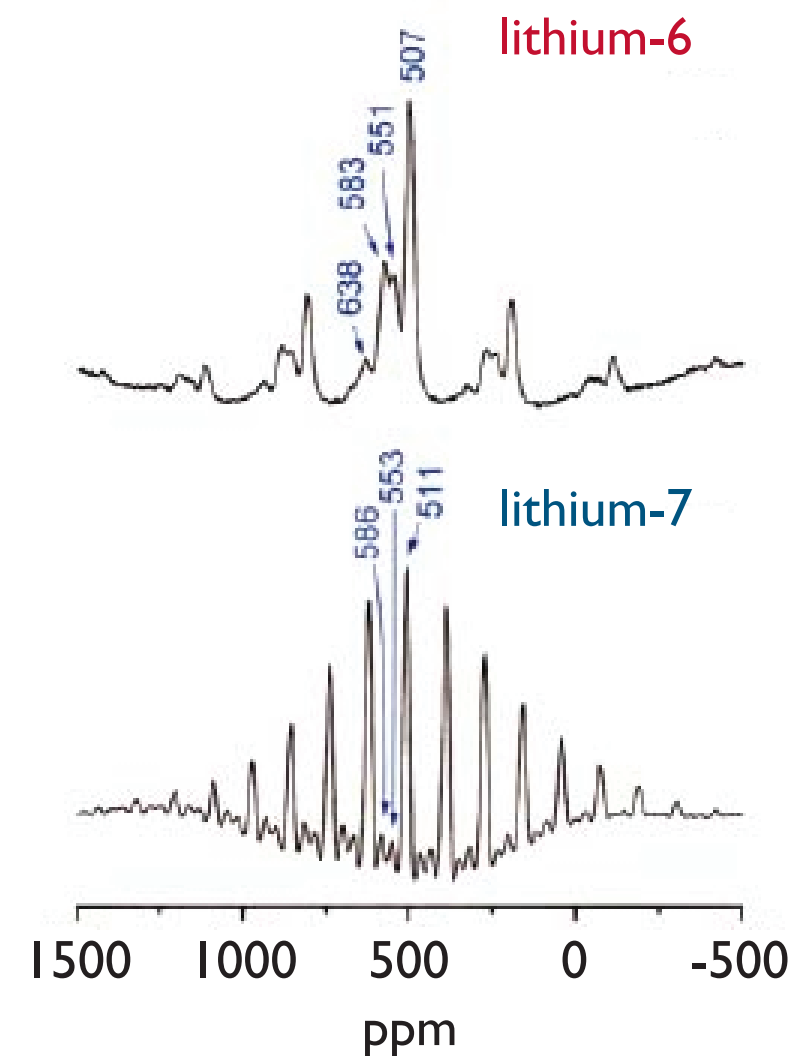
Lithium-7

- ★ The spectrum is dominated by the quadrupolar interaction and the dipolar couplings, resulting in a broad set of spinning sidebands.

Lithium-6

- ★ The low magnetogyric ratio and quadrupole moment result in better resolution of different local Li environments.

	^6Li	^7Li
Natural abundance / %	7	93
Spin	1	3/2
Magnetogyric ratio / $\text{rad s}^{-1} \text{T}^{-1}$	3.94×10^7	10.4×10^7
Quadrupole moment	-8×10^{-4}	-4×10^{-2}



Electron-nucleus interactions

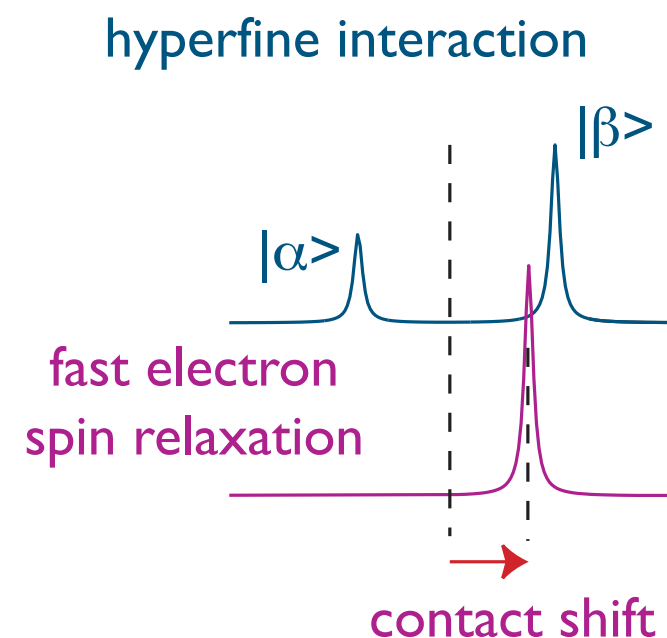
Unpaired electrons (in metals, paramagnetic materials etc.) result in an electronic magnetic moment which can interact with the nuclear spin via the hyperfine coupling.

- ★ The hyperfine interaction causes a splitting in the NMR spectrum.
- ★ Because the electronic Zeeman levels are widely spaced in energy, the Boltzmann population of the lower level (the $|\beta\rangle$ state) far exceeds that of the upper level (the $|\alpha\rangle$ state), so the corresponding line in the NMR spectrum is of higher intensity.
- ★ Fast electron spin-lattice relaxation makes the NMR lines coalesce and the frequency of the coalesced line is an average weighted by the electronic Zeeman populations.
- ★ This results in the **contact shift**.

Hyperfine coupling constant

$$\delta = \frac{A}{h\nu_0} \langle S_z \rangle$$

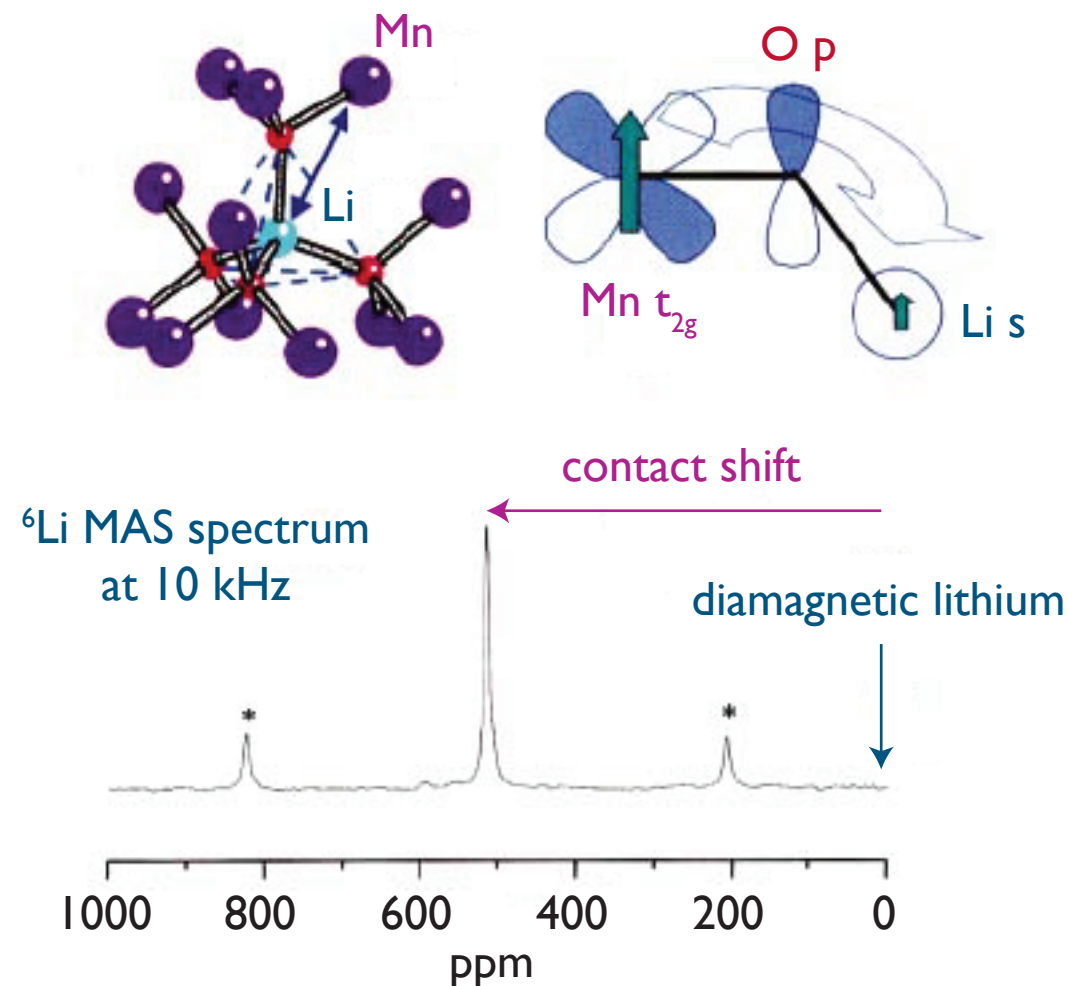
Contact shift Electron polarization



Correlation with structure in LiMn_2O_4 spinels

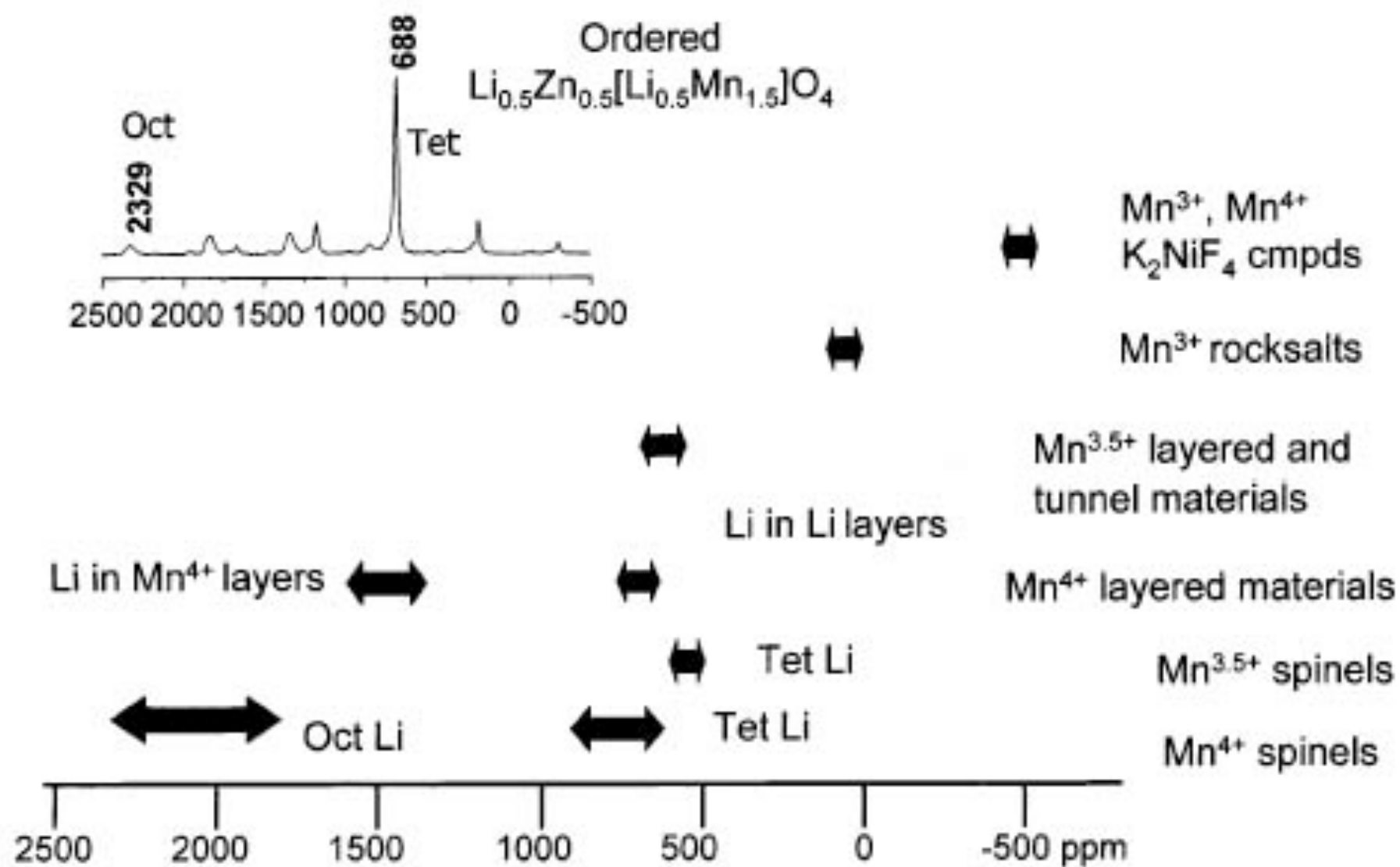
Example: LiMn_2O_4 synthesized at 1123 K

- ★ Lithium manganate spinels have been proposed as alternative cathode materials.
- ★ The Li atoms are tetrahedrally co-ordinated by O with 12 nearest neighbor Mn atoms.
- ★ The hyperfine coupling between the unpaired electron in the Mn t_{2g} orbital and the Li nucleus is mediated via a 2p orbital on the bridging O.
- ★ This results in a 520 ppm shift.



Lithium local environments in Li-Mn compounds

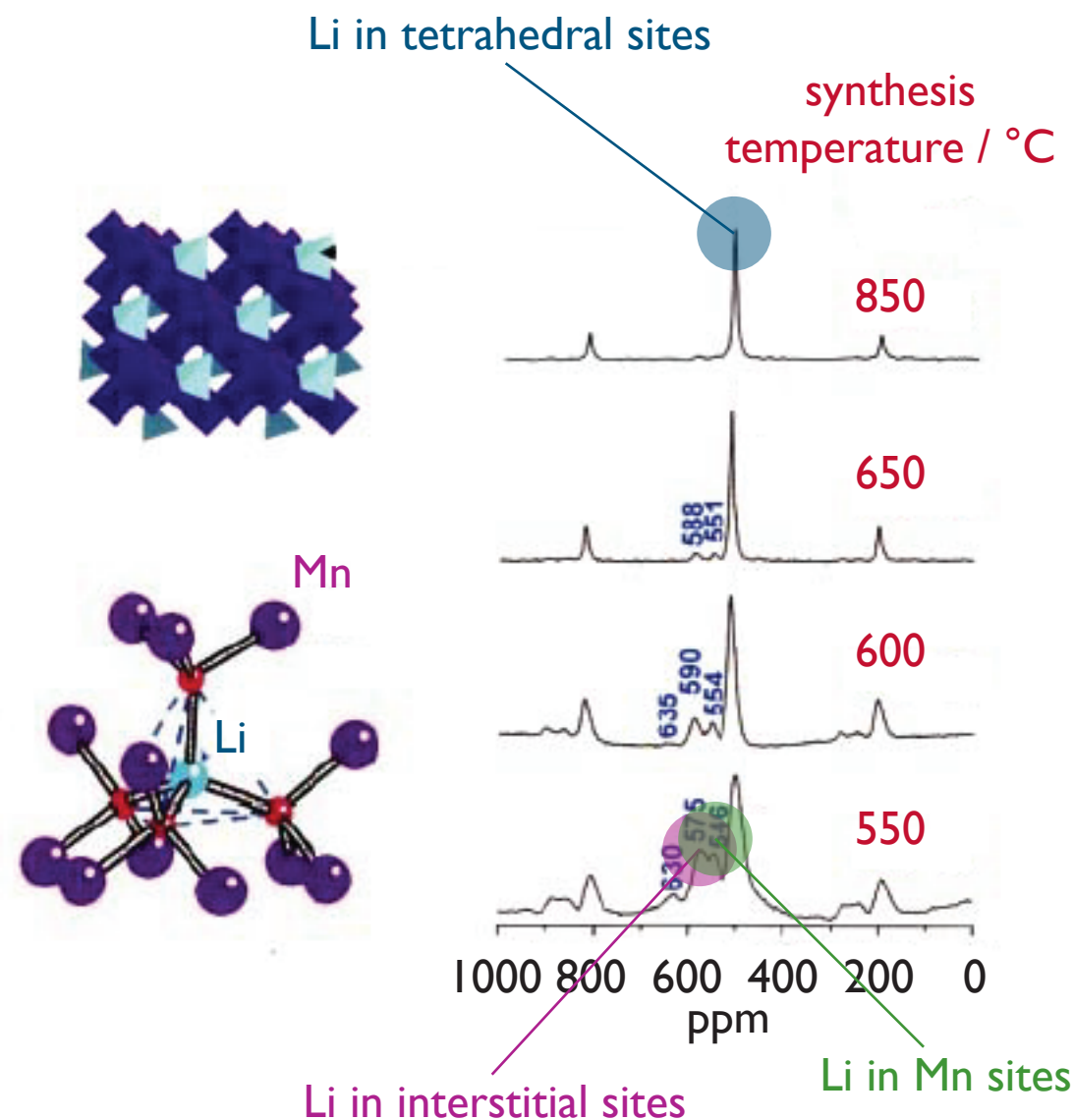
The contact shift can be used like the chemical shift to establish local Li environments.



Defect structure of “LiMn₂O₄” spinels

Example: “LiMn₂O₄” spinels synthesized at different temperatures.

- ★ the crystal structure is consistent with **one** Li site as observed with NMR of samples synthesized at high temperatures.
- ★ when synthesized at lower temperature the material has a defect structure Li[Mn_{1.95}Li_{0.05}]O₄ which is thought to promote stability over many charge/discharge cycles.



“Universal dynamical behaviour” for Li⁺ conductors

Examples: $\text{Li}_{4-3x}\text{Ga}_x\text{GeO}_4$, $\text{Li}_3\text{Sc}(\text{PO}_4)_3$, $\text{Li}_9\text{B}_{19}\text{S}_{33}$, $\text{Li}_{4-2x}\text{Sr}_{2+x}\text{B}_{10}\text{S}_{19}$

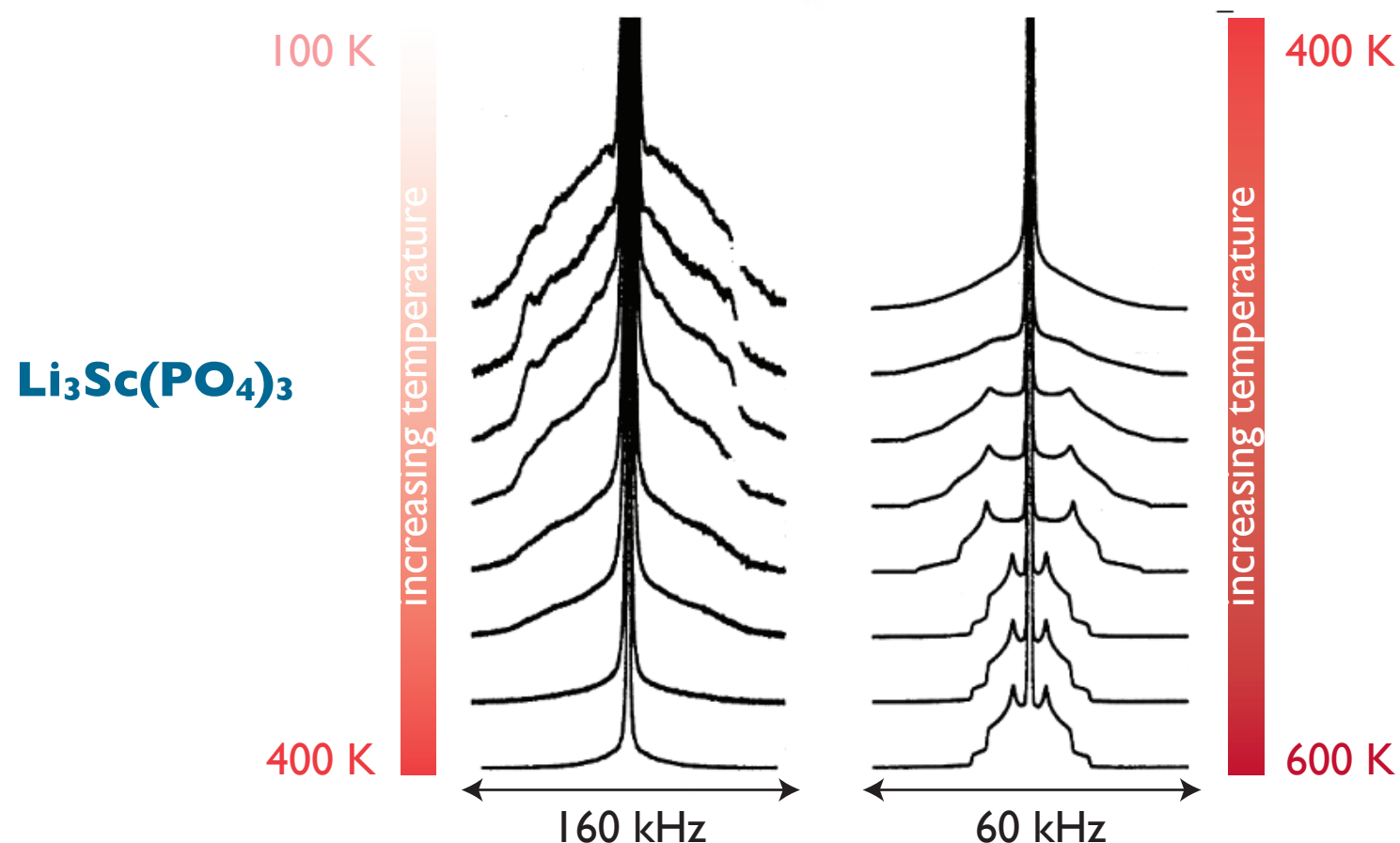
These materials have a disordered lithium sub-lattice with a large surplus of available sites.

At low temperatures: rigid lattice spectra show quadrupolar satellites smeared out by a distribution of electric field gradients at the lithium sites.

At higher temperatures: corresponding to the onset of lithium ion dynamics a line narrowing process starts and the central line becomes Lorentzian.

At high temperatures: there is a well-defined extreme narrowing spectrum with an averaged C_Q indicating an anisotropic motion.

Spin-lattice relaxation is governed by quadrupolar interactions, but the linewidth is dipolar in origin.



R. Bertermann and W. Müller-Warmuth, *Z. Naturforsch.* **53a**, 863 (1998.)

Exchange NMR of $\text{Li}[\text{Mn}_{1.96}\text{Li}_{0.04}]\text{O}_4$

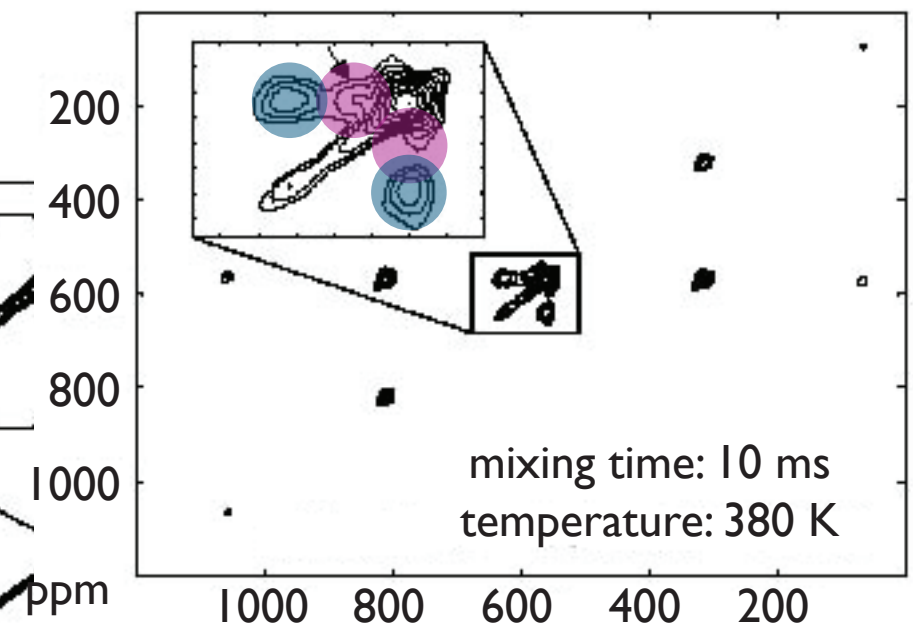
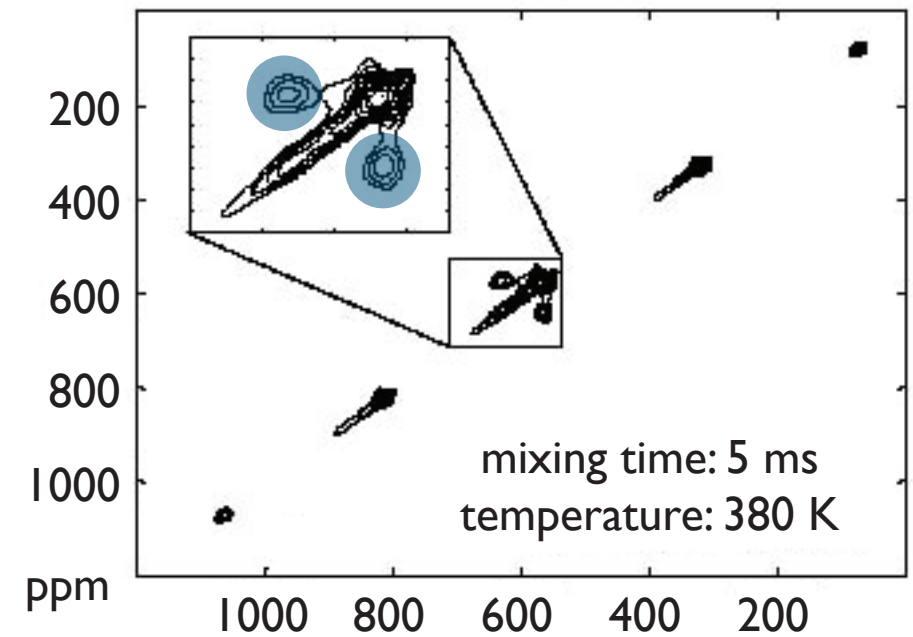
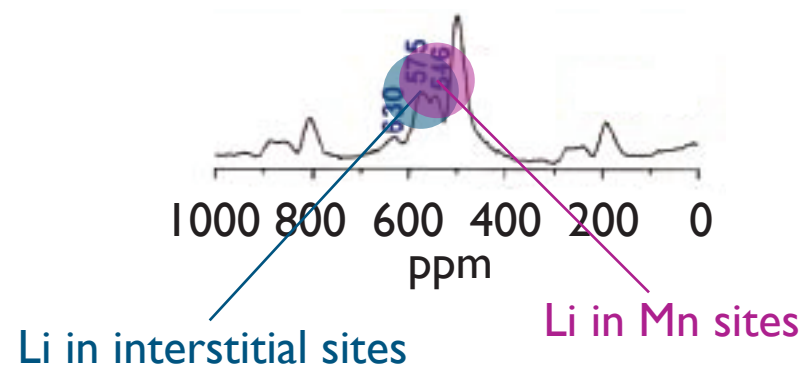
Lithium-7 MAS 2D exchange NMR allows diffusion timescales and pathways to be identified.

At 280 K there is no off-diagonal intensity, indicating that any diffusion process has a correlation time of longer than 5 ms at this temperature.

At 380 K cross peaks appear which at shorter mixing times link Li ions in the usual tetrahedral sites with interstitial Li ions

At longer mixing times the Li ions in the Mn sites also start to take part in diffusion.

The diffusion mechanism involves occupation of the interstitial sites.



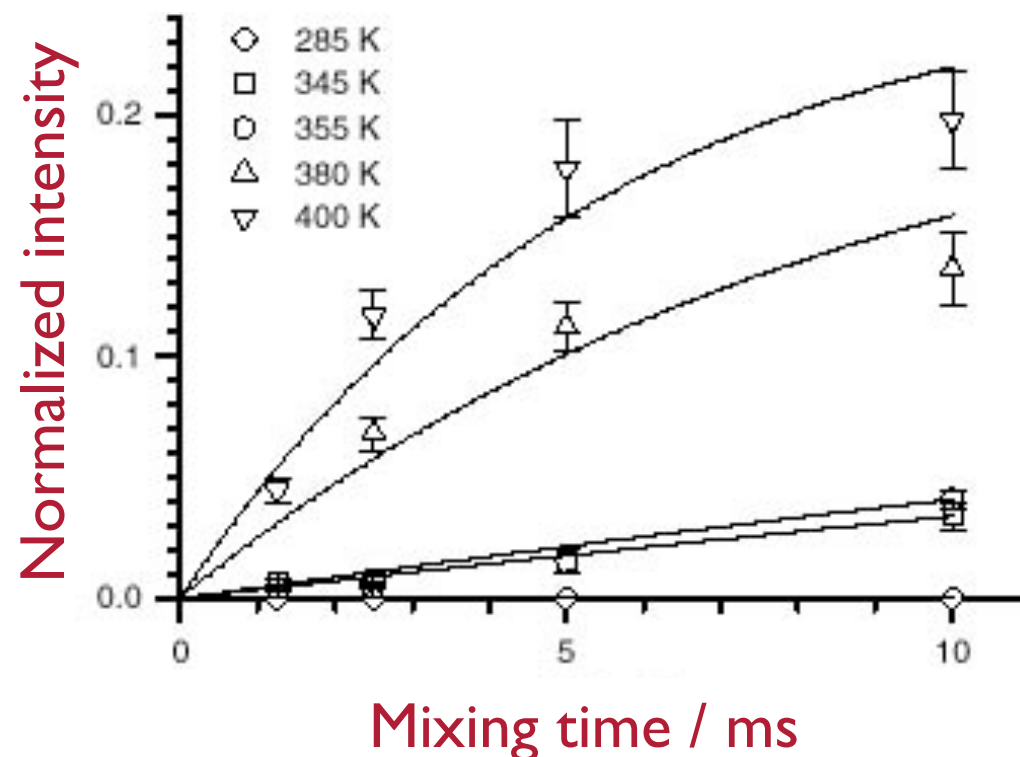
Exchange NMR of $\text{Li}[\text{Mn}_{1.96}\text{Li}_{0.04}]\text{O}_4$

The **build-up** of the cross peak intensities with mixing time allows measurement of:

- ★ **correlation times** τ_c which can be equated to the time between Li^+ hops between interstitial and tetrahedral sites
- ★ **activation energies** for ion hopping
- ★ **diffusion coefficients** since these are related to correlation times via:

$$D = \frac{l d^2}{4 \tau_c}$$

where d is the distance covered in one hop



Lithium nitride

- ★ hexagonal layered crystal structure with space group P6/mmm
- ★ highest reported Li⁺ ion conductivity in a crystalline material
- ★ conductivity and diffusion is anisotropic:

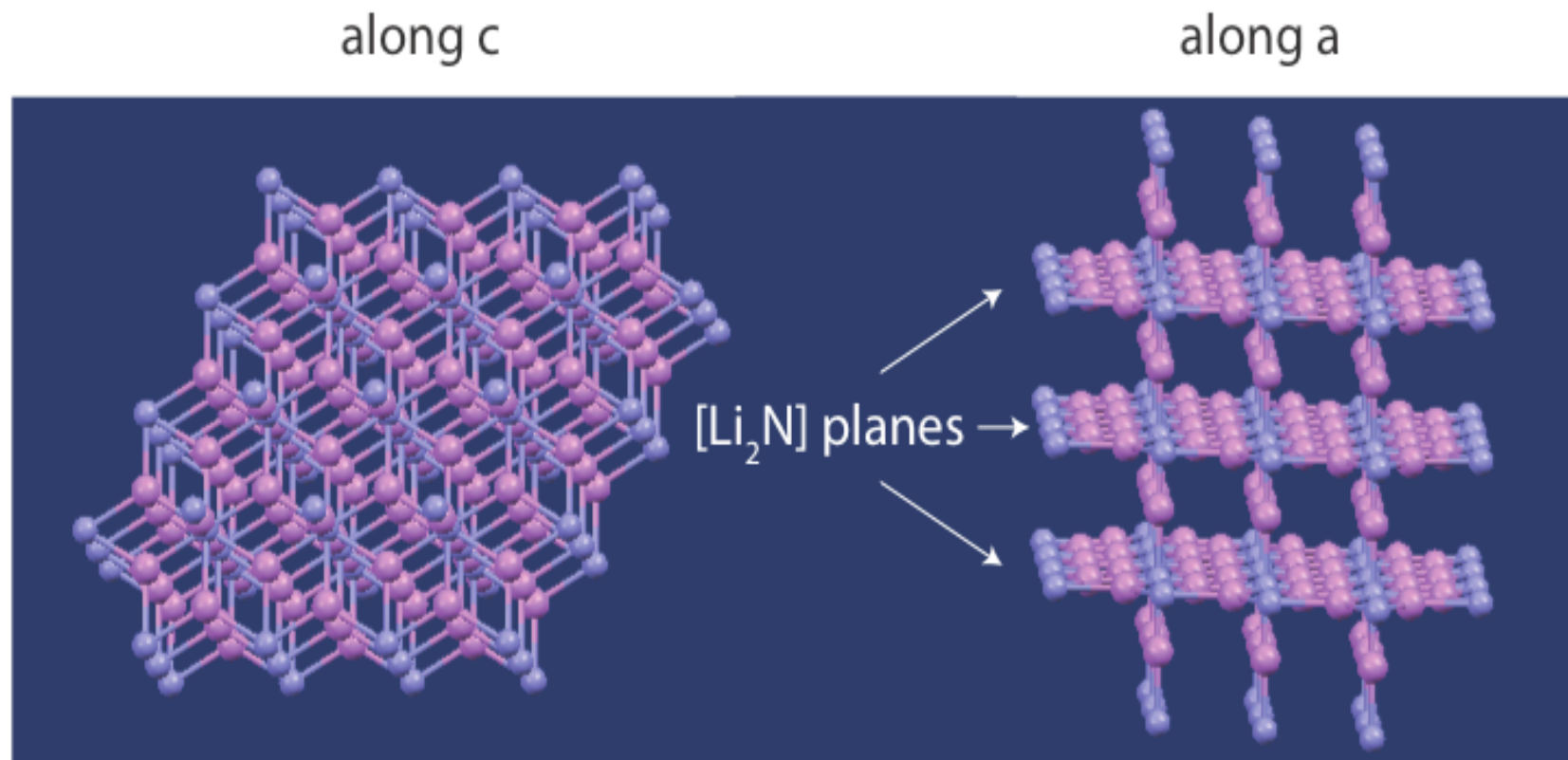
intra-layer

$$\sigma = 1 \times 10^{-3} \text{ S cm}^{-1} (E_a = 0.1 - 0.3 \text{ eV}) \text{ perpendicular to } c$$

inter-layer

$$\sigma = 1 \times 10^{-5} \text{ S cm}^{-1} (E_a = 0.49 \text{ eV}) \text{ parallel to } c$$

- ★ 1-2 % Li(2) vacancies in the [Li₂N] *ab* planes are responsible for the intra-layer contribution



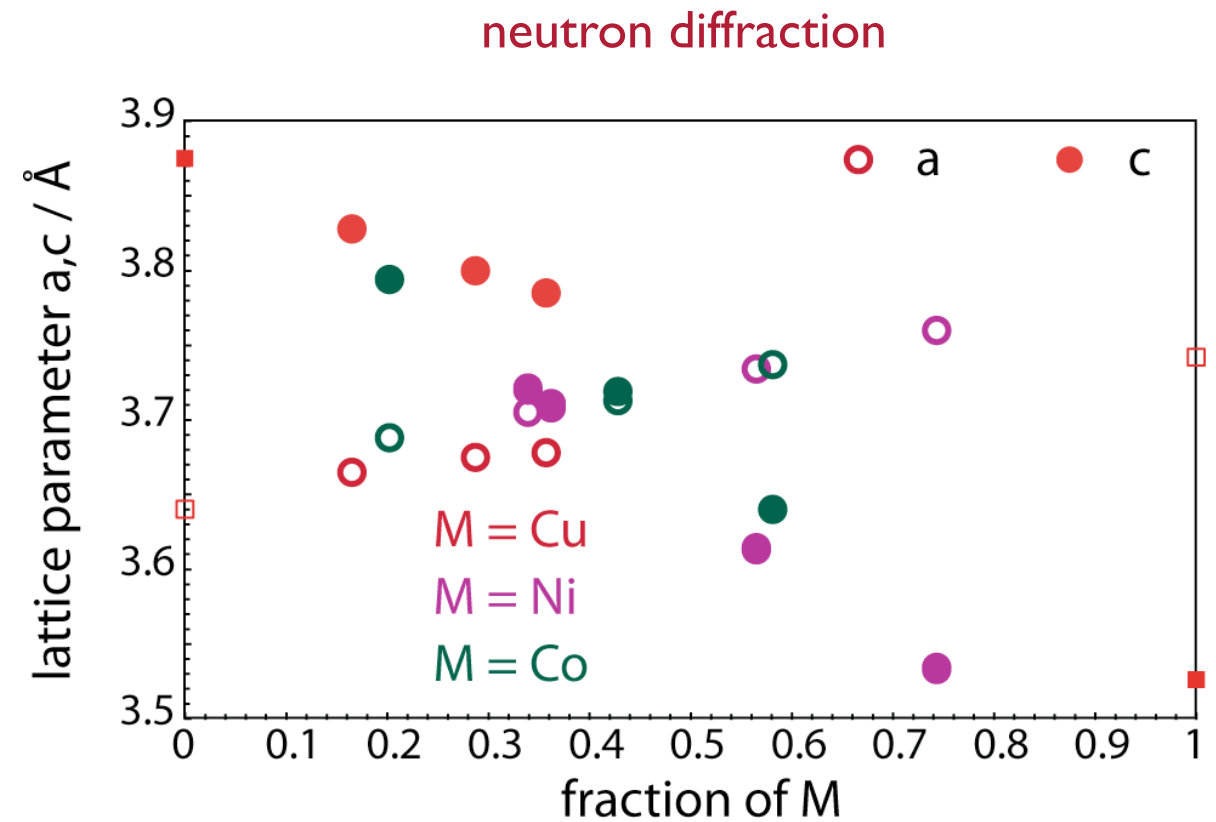
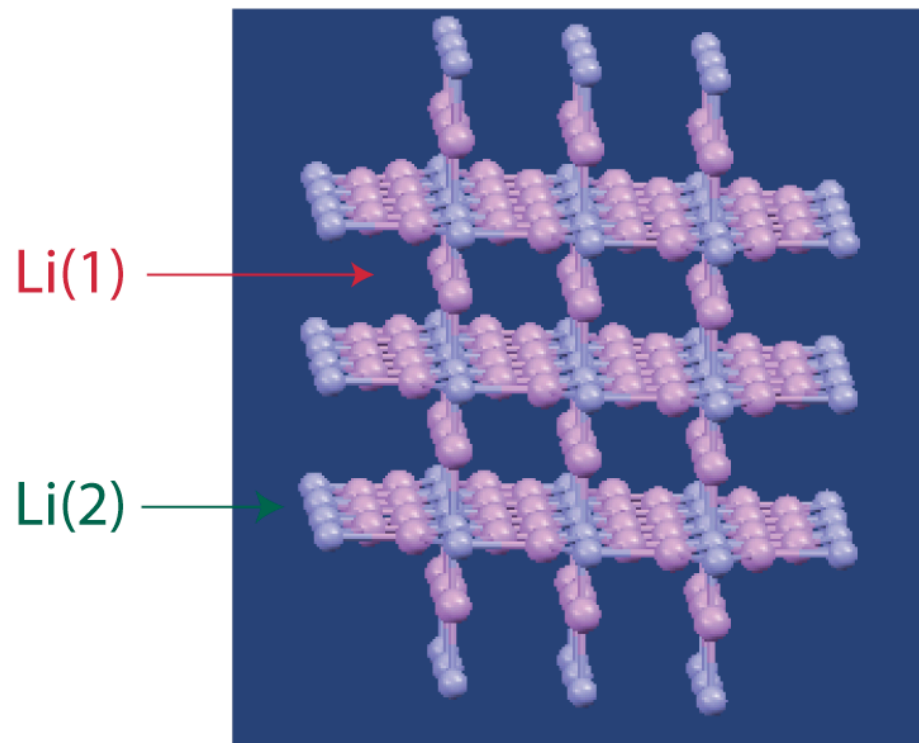
Layered metallonitrides

- ★ ternary transition metal substituted nitrides $\text{Li}_{3-x-y}\text{M}_x\text{N}$; $\text{M} = \text{Cu}, \text{Ni}, \text{Co}$.

D. H. Gregory, P. M. O'Meara, A. G. Gordon, J. P. Hodges, S. Short and J. D. Jorgensen, *Chem. Mater.*, **14**, 2063 (2002).

- ★ Li_3N structure retained; M in Li(I) sites; vacancies in the $[\text{Li}_2\text{N}]$ plane are disordered.
- ★ $\text{Li}_{2.6}\text{Co}_{0.4}\text{N}$ has been proposed as an anode material.

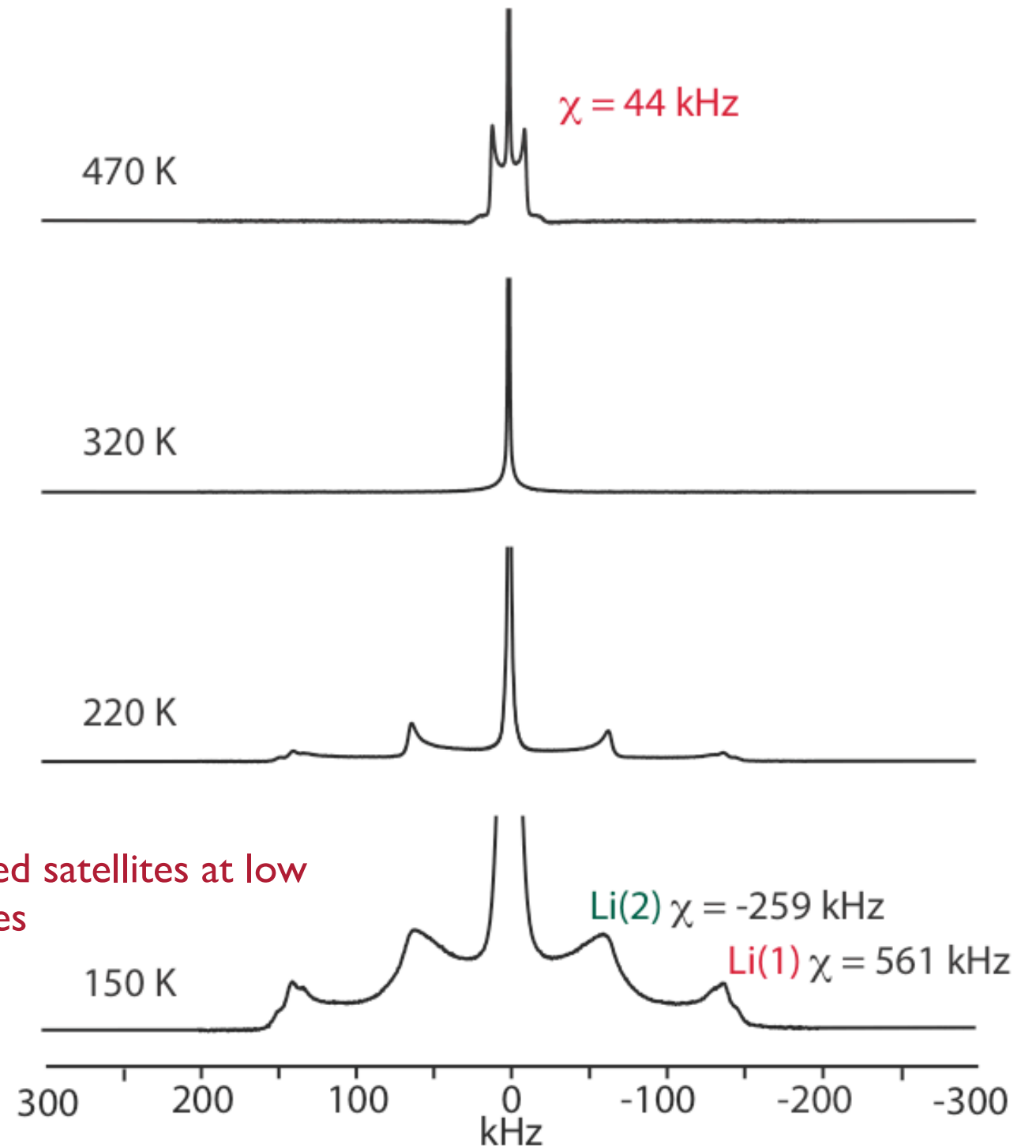
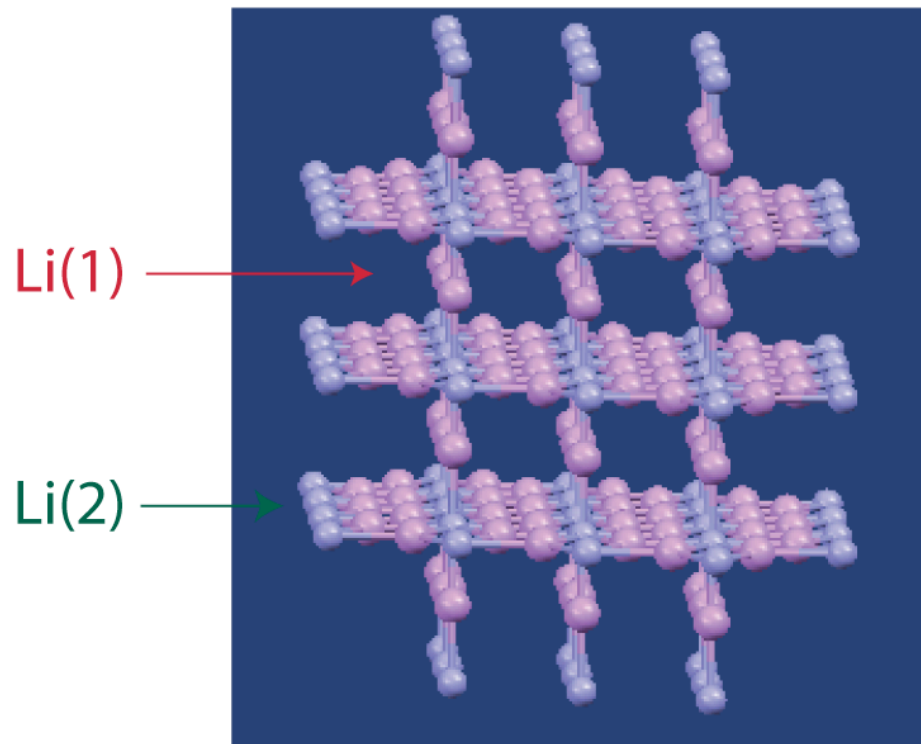
T. Shodai, S. Okada, S. Tobishima, J. Yamaki, *Solid-State Ionics*, **86-88**, 785 (1996).



$\text{Li}_{3-x-y}\text{Cu}_x\text{N}$

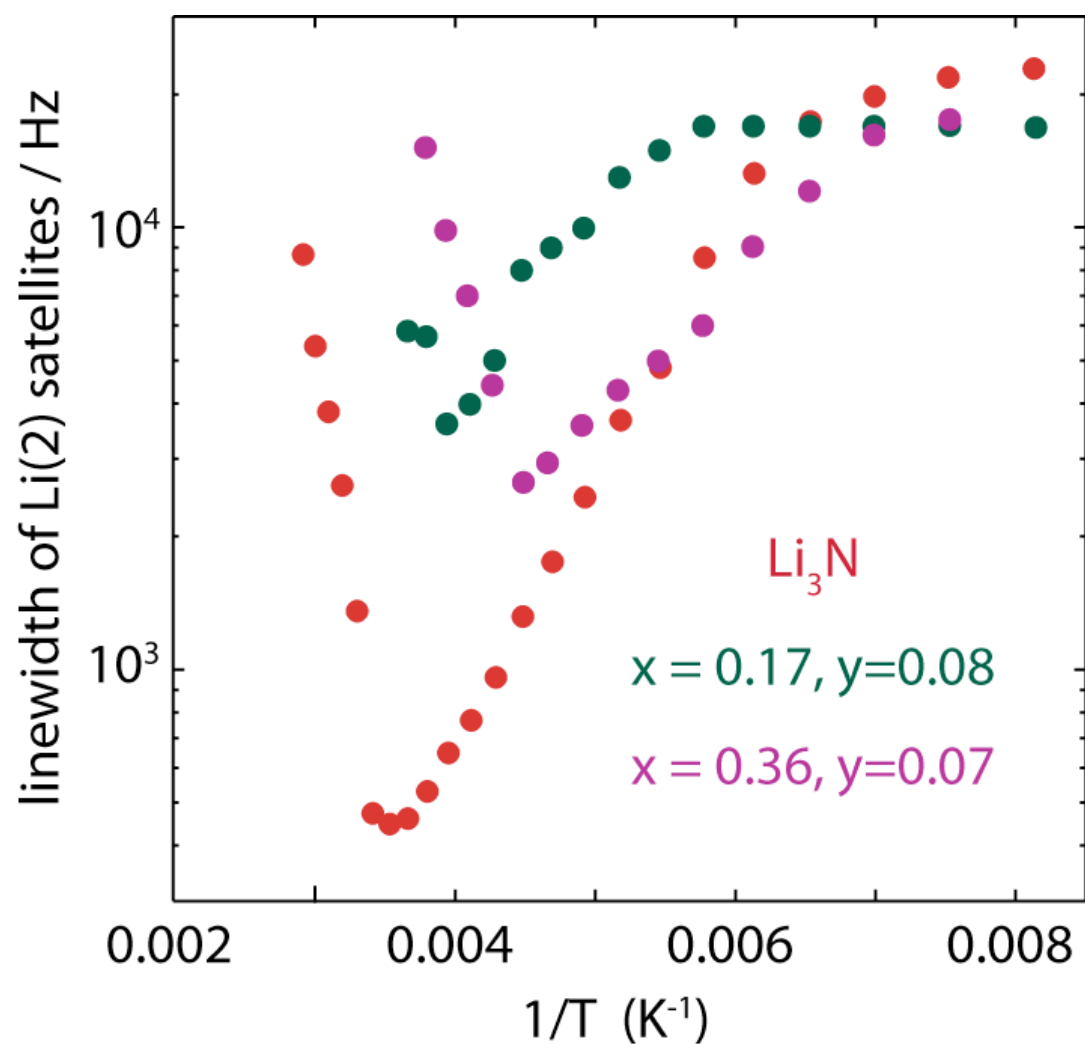
- ★ $x < 0.4$; low vacancy concentration
- ★ diamagnetic

wideline lithium-7 spectra
 $x = 0.29, y = 0.07$

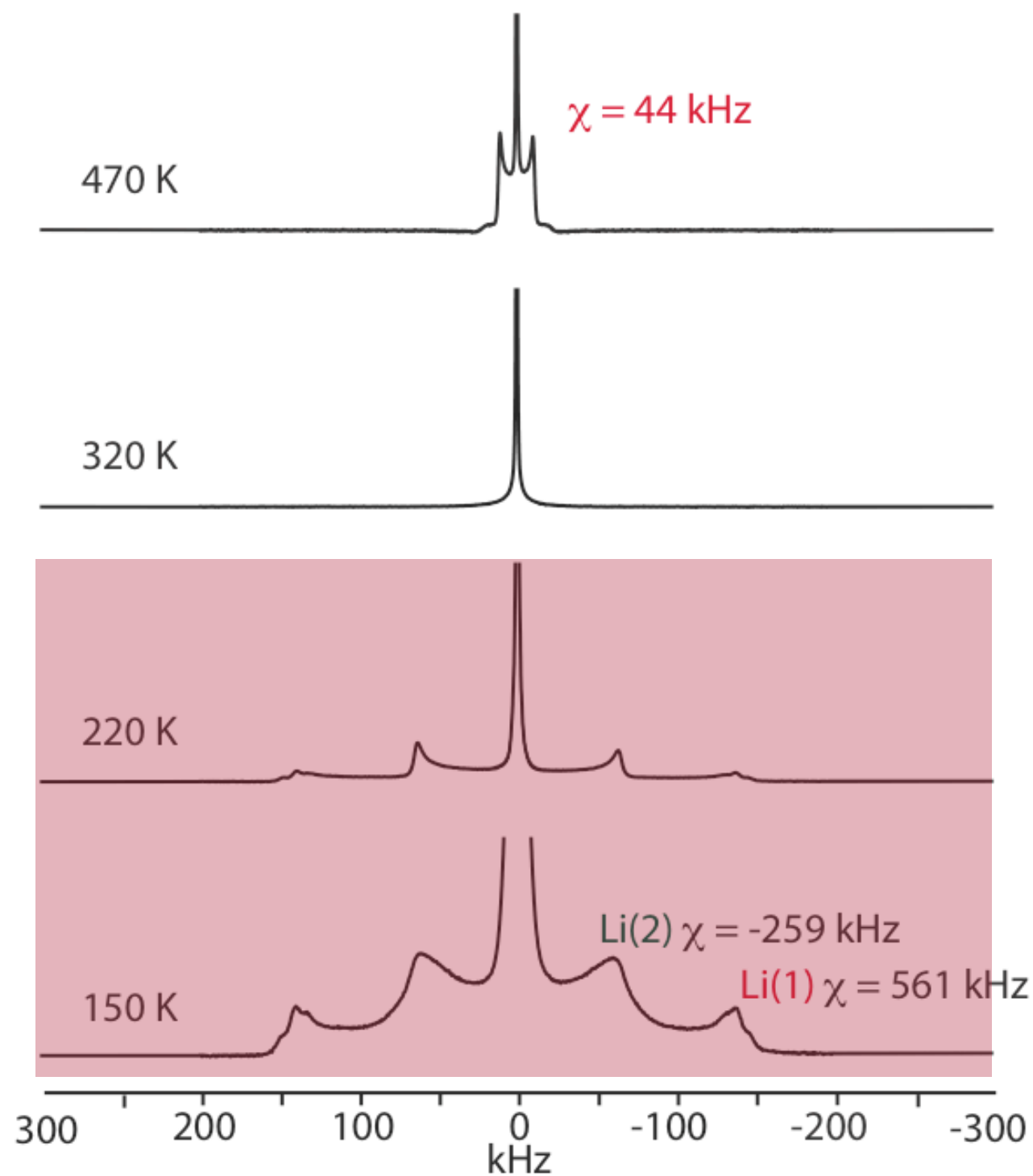


two sets of dipolar-broadened satellites at low temperatures

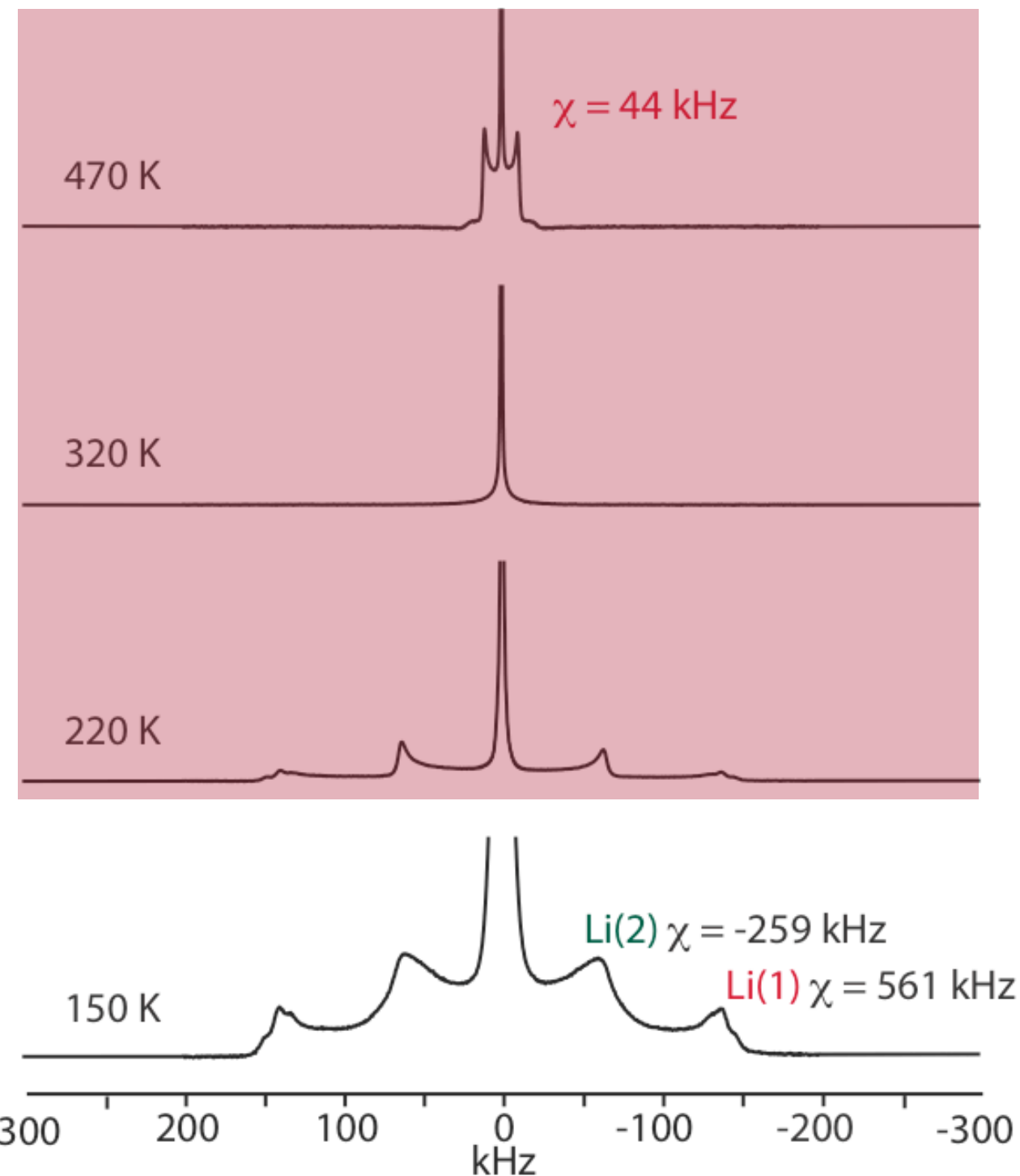
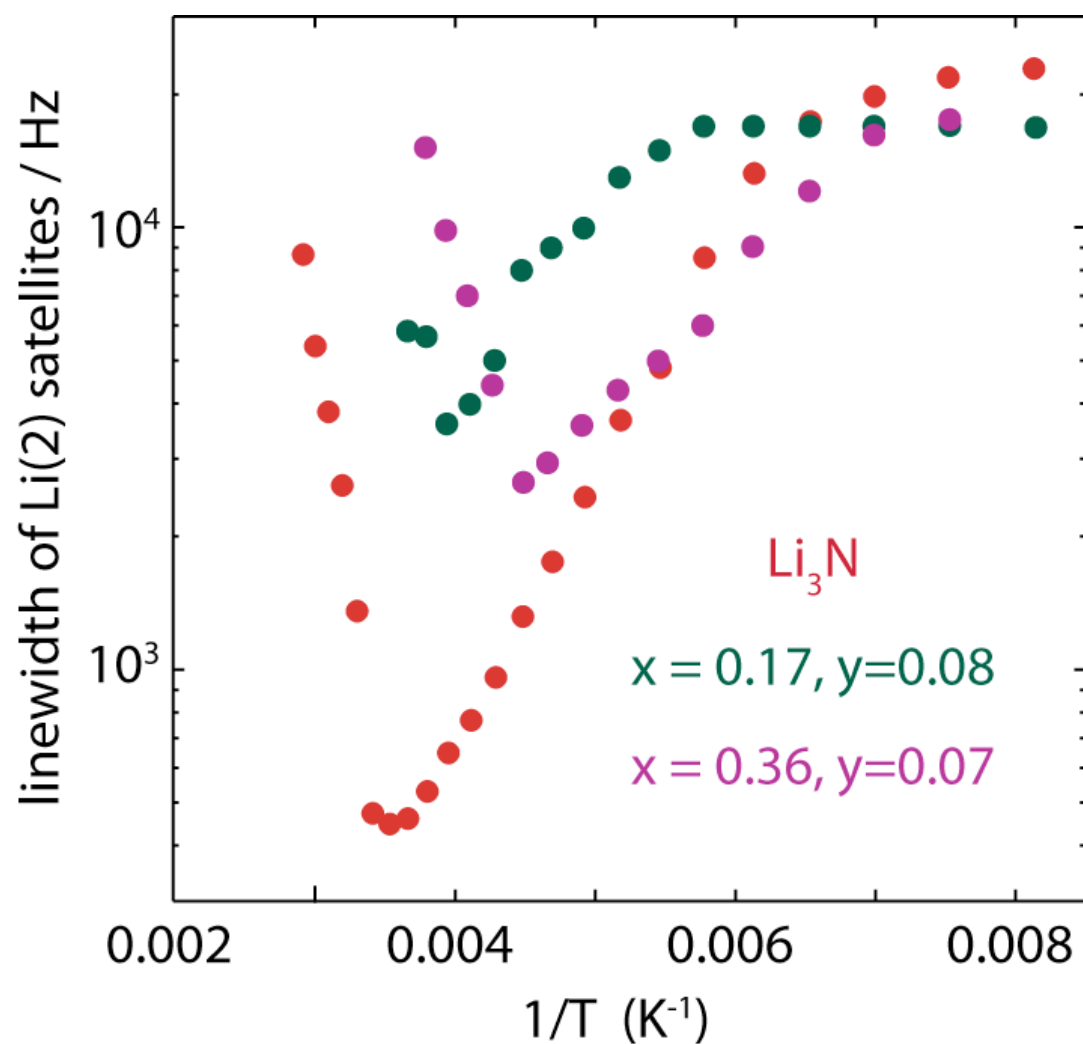
$\text{Li}_{3-x-y}\text{Cu}_x\text{N}$:VT wideline NMR



motional narrowing of dipolar broadened satellites, particularly Li(2) due to intra-layer diffusion

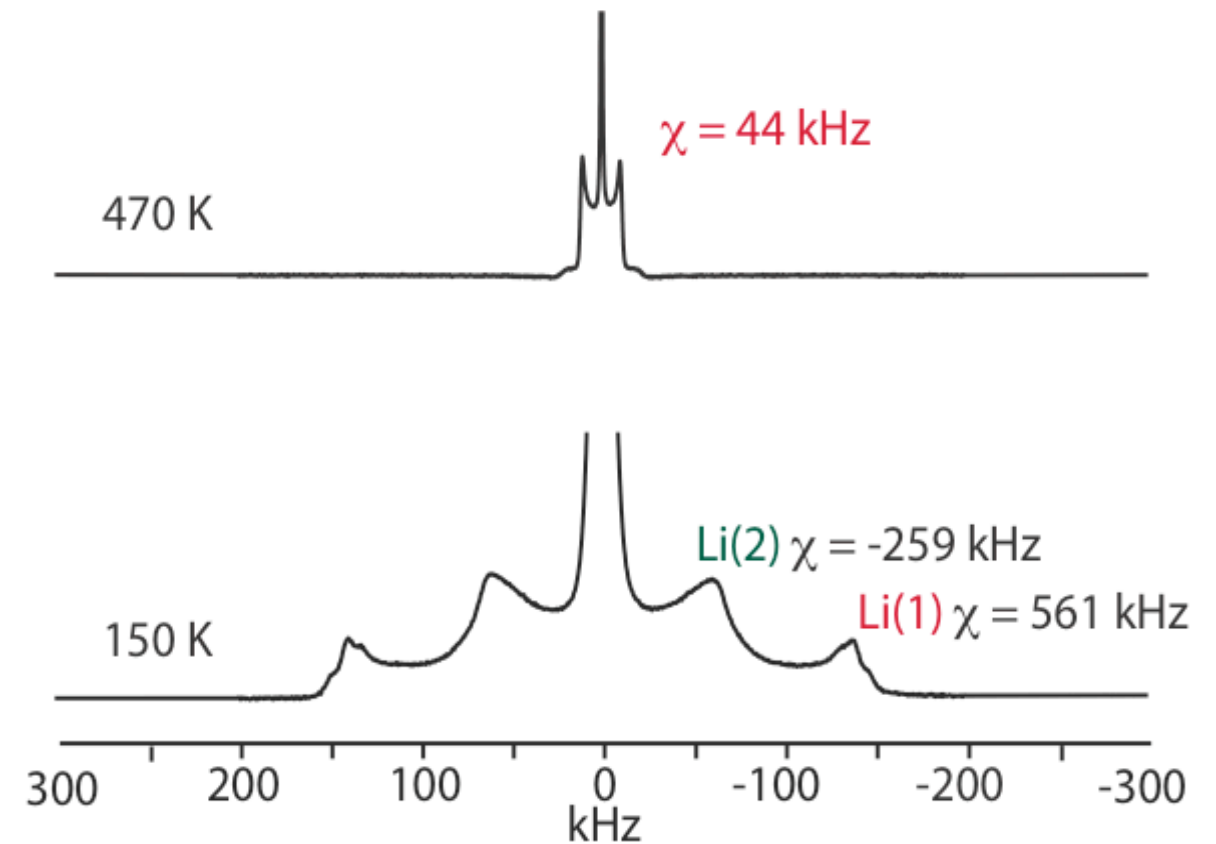
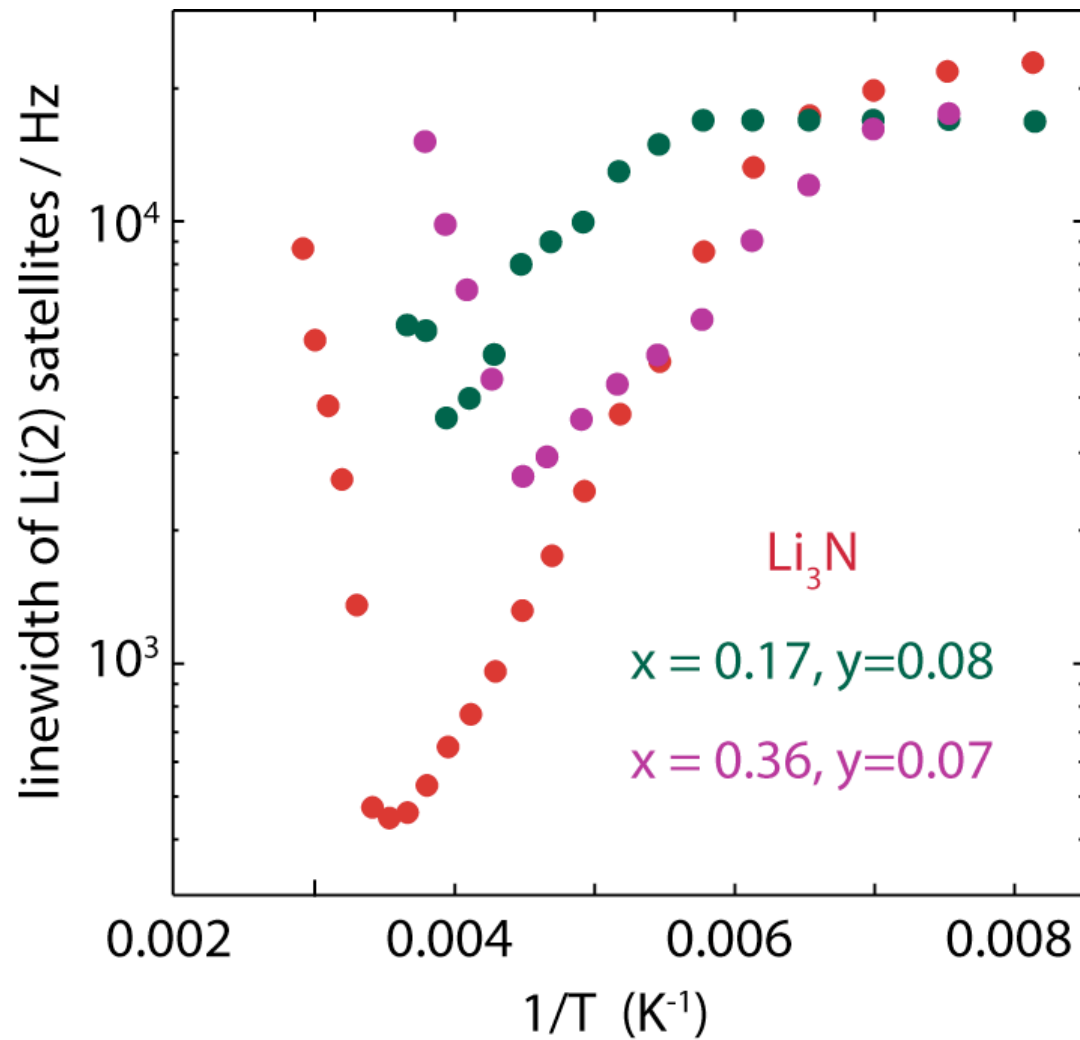


$\text{Li}_{3-x-y}\text{Cu}_x\text{N}$:VT wideline NMR



**exchange broadening of both satellites,
suggests an exchange mechanism for inter-
layer diffusion**

Inter-layer diffusion in $\text{Li}_{3-x-y}\text{Cu}_x\text{N}$



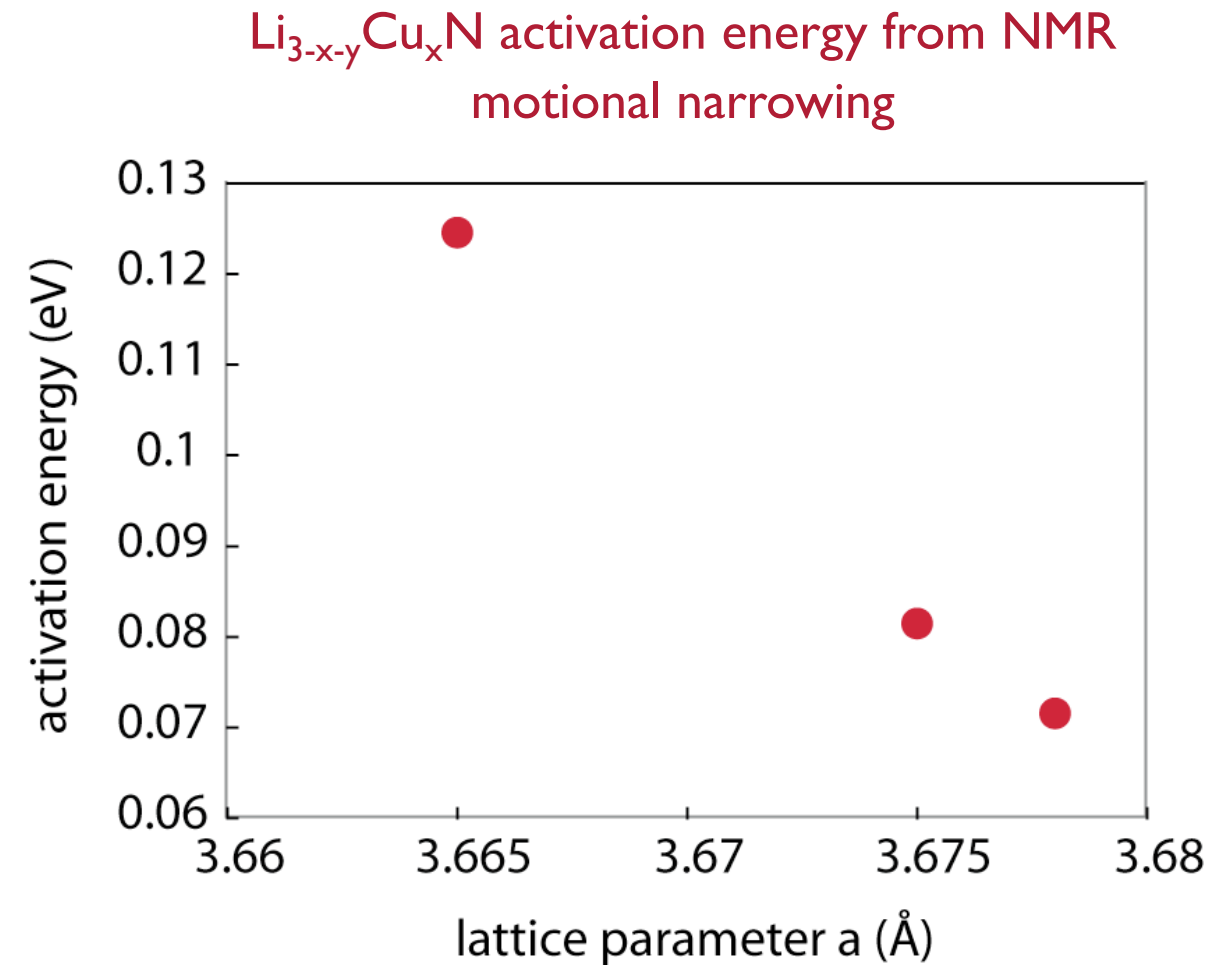
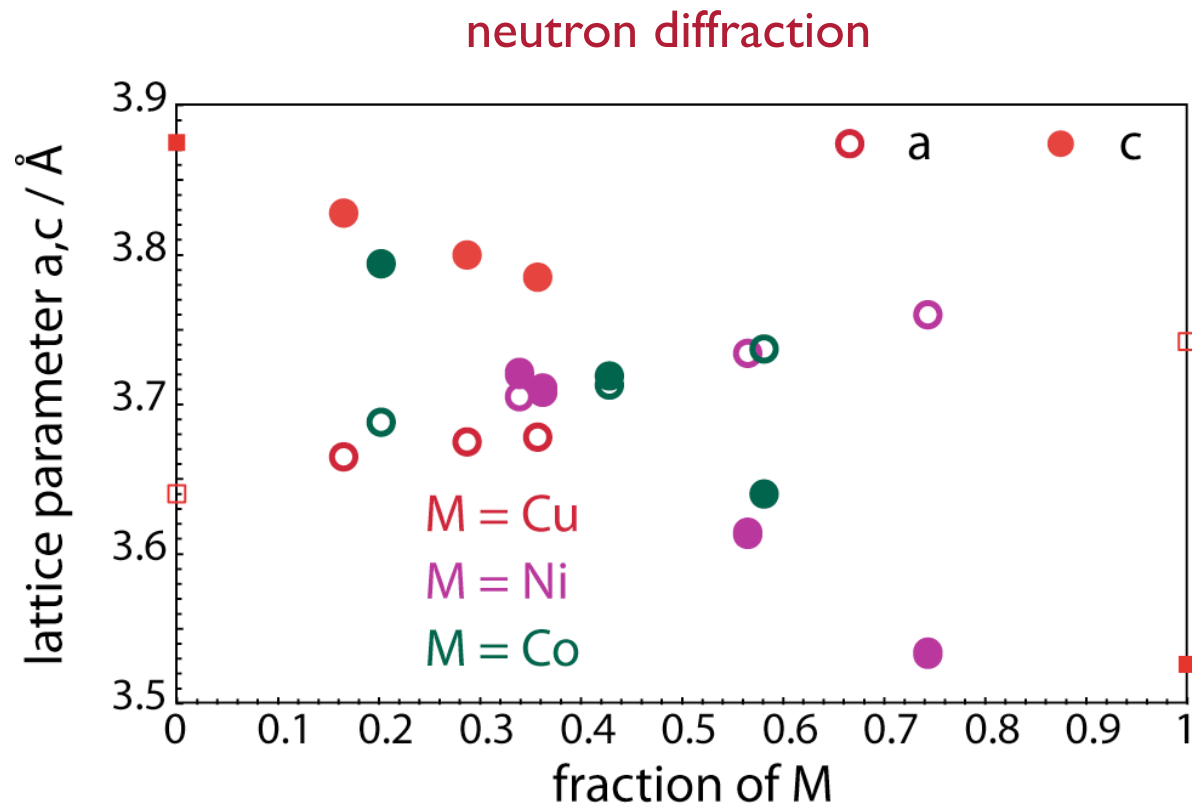
onset of inter-layer diffusion at lower temperatures cf. Li_3N

average value of C_Q suggests Cu enters the $[\text{Li}_2\text{N}]$ layers at high T

Intra-layer diffusion in $\text{Li}_{3-x-y}\text{Cu}_x\text{N}$

As x increases:

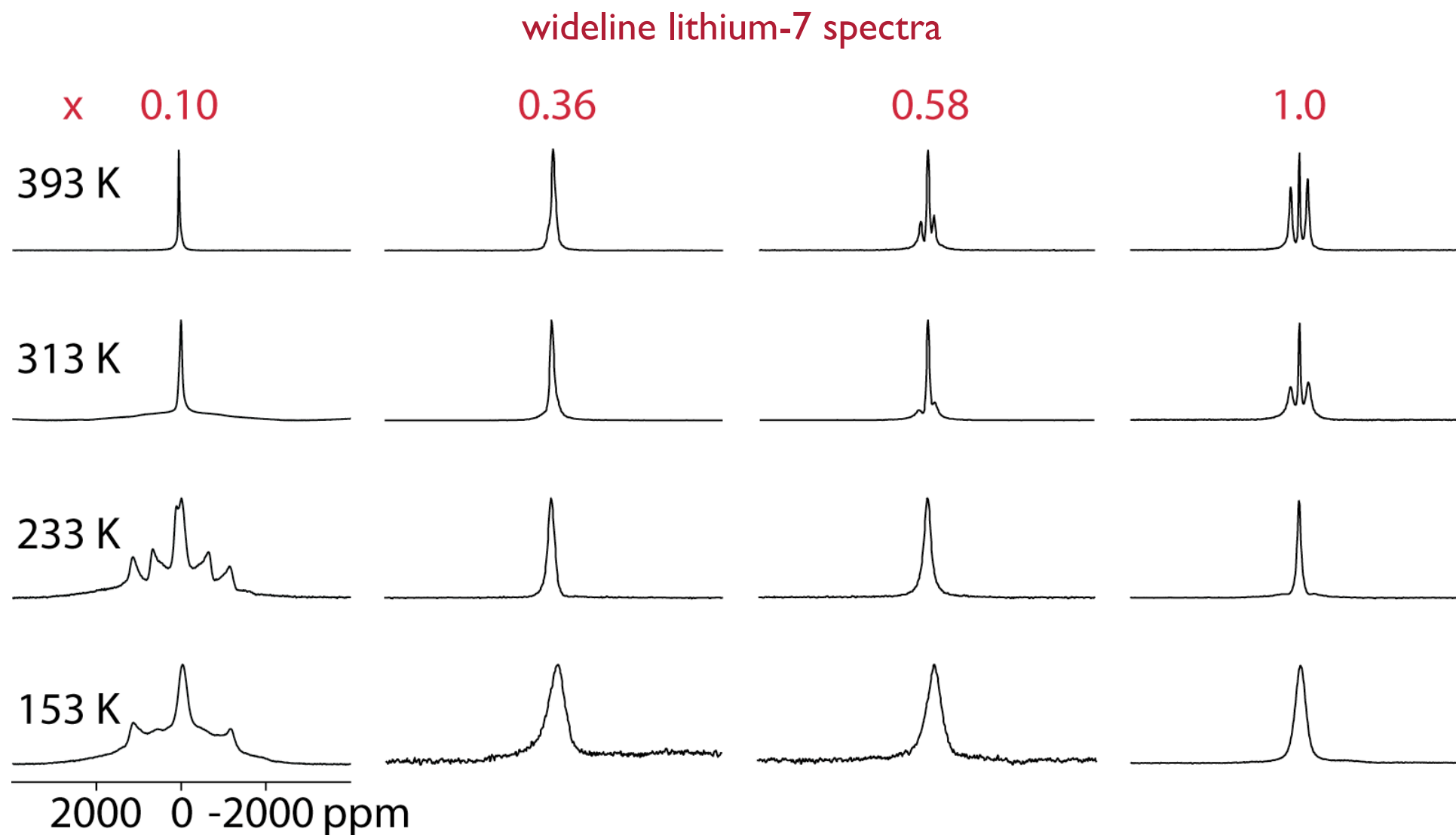
- ★ a **lengthens** - more open framework - lowers E_a
- ★ c **shortens** - less polar, more covalent framework - raises E_a



E_a decreases as a lengthens

$\text{Li}_{3-x-y}\text{Ni}_x\text{N}$

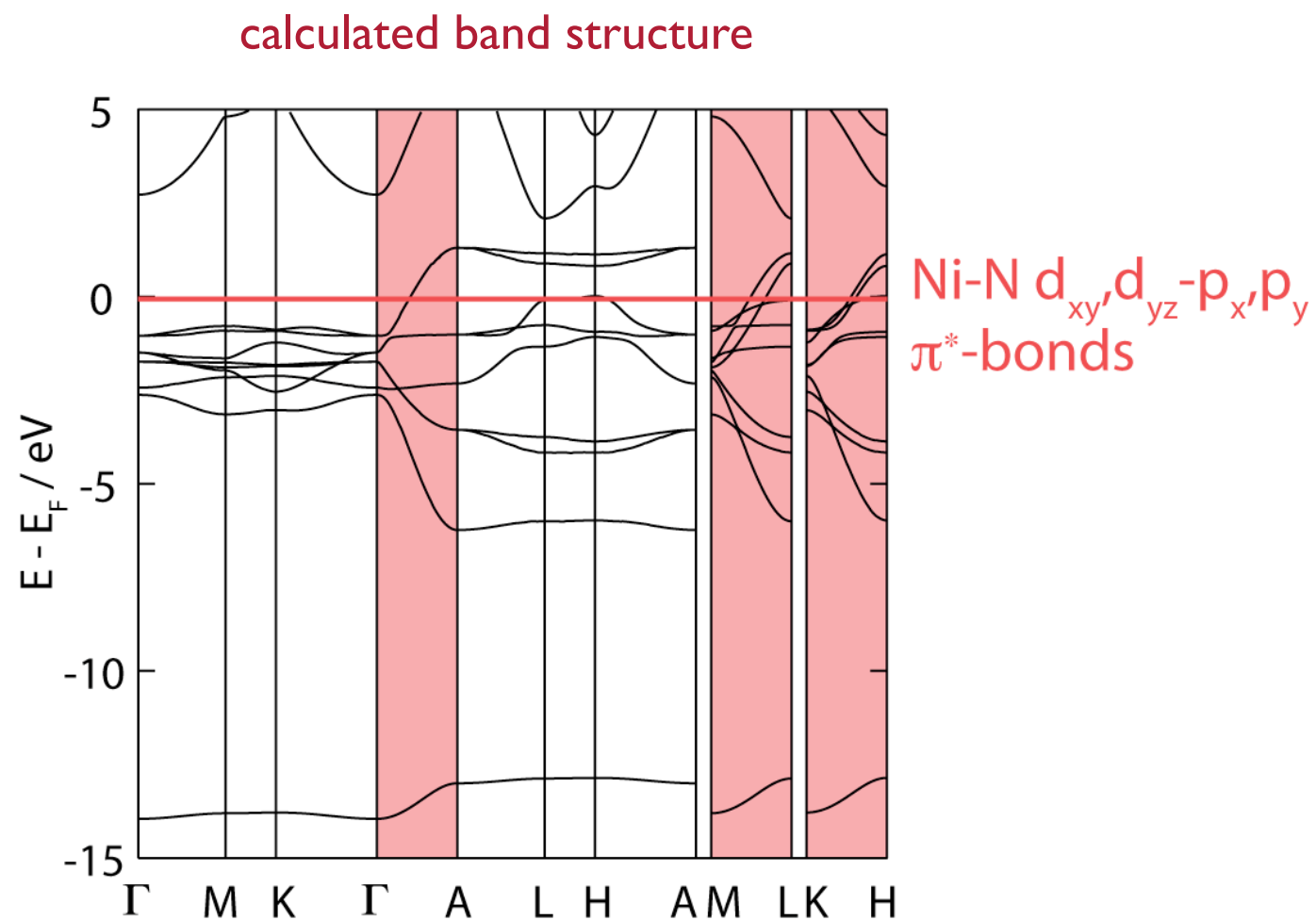
- ★ $x < 1$; higher vacancy concentrations
- ★ weakly paramagnetic or metallic



transition to ordered vacancies
no evidence of inter-layer diffusion below 500 K, even for small x
“universal dynamical behavior” at high x

LiNiN: band structure

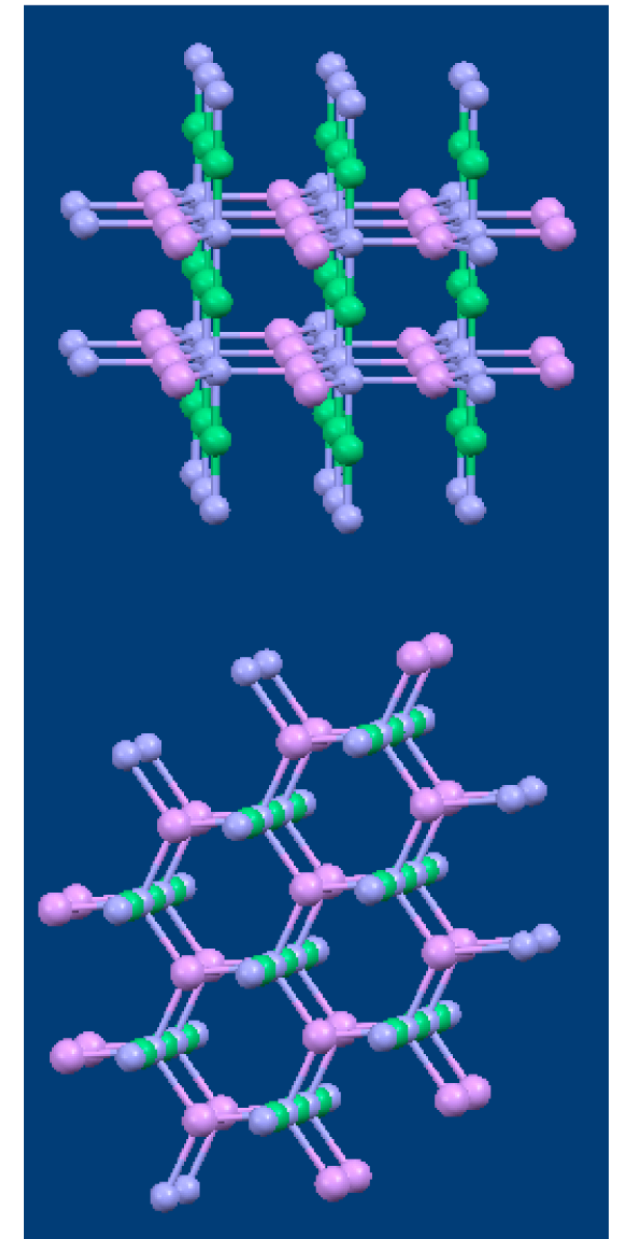
- ★ new structure with a supercell; vacancies in the $[\text{Li}_2\text{N}]$ plane are ordered
- ★ I-D metal due to linear N-Ni-N chains along c axis
- ★ combined with intra-layer Li^+ ion conductivity



bands which cross E_F do so along the c axis

neutron diffraction

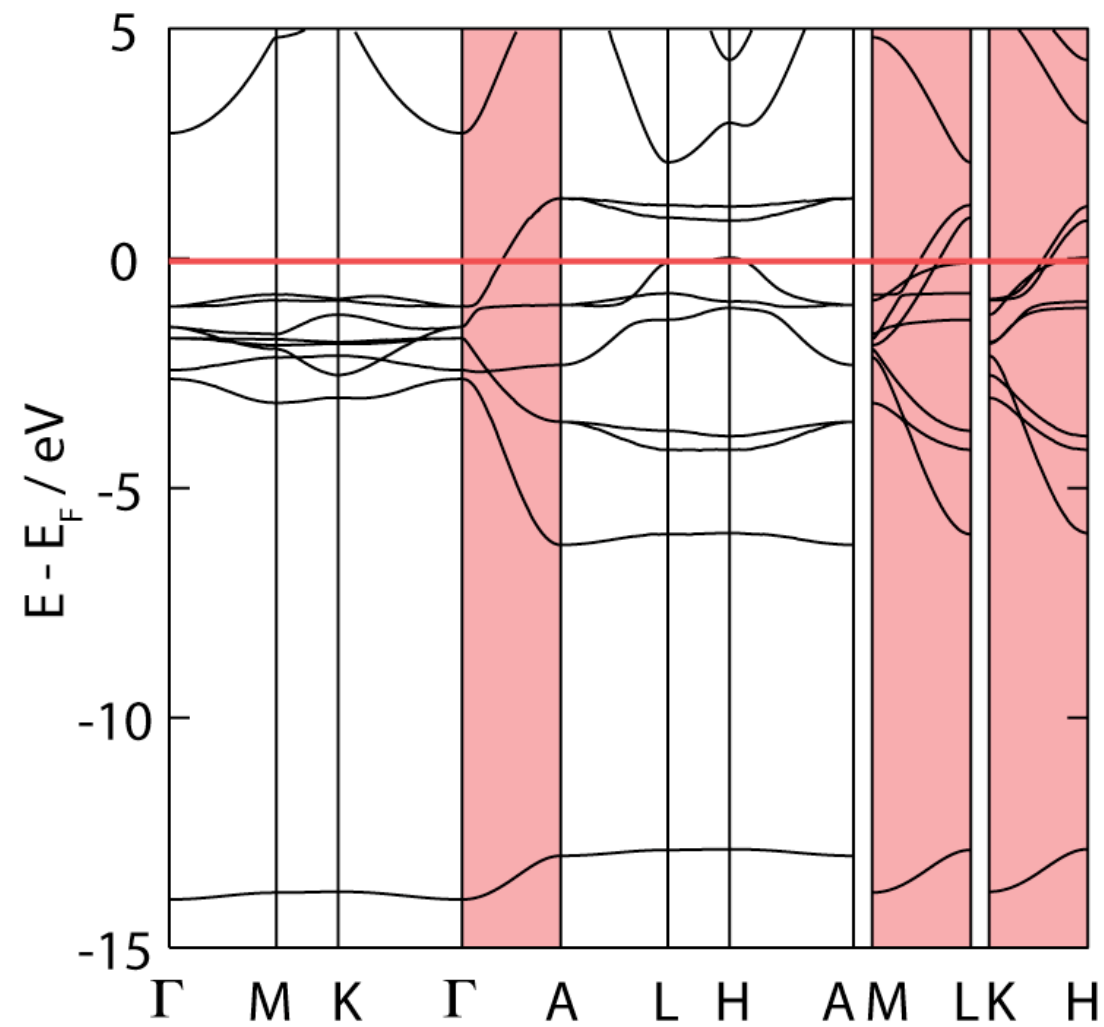
along b



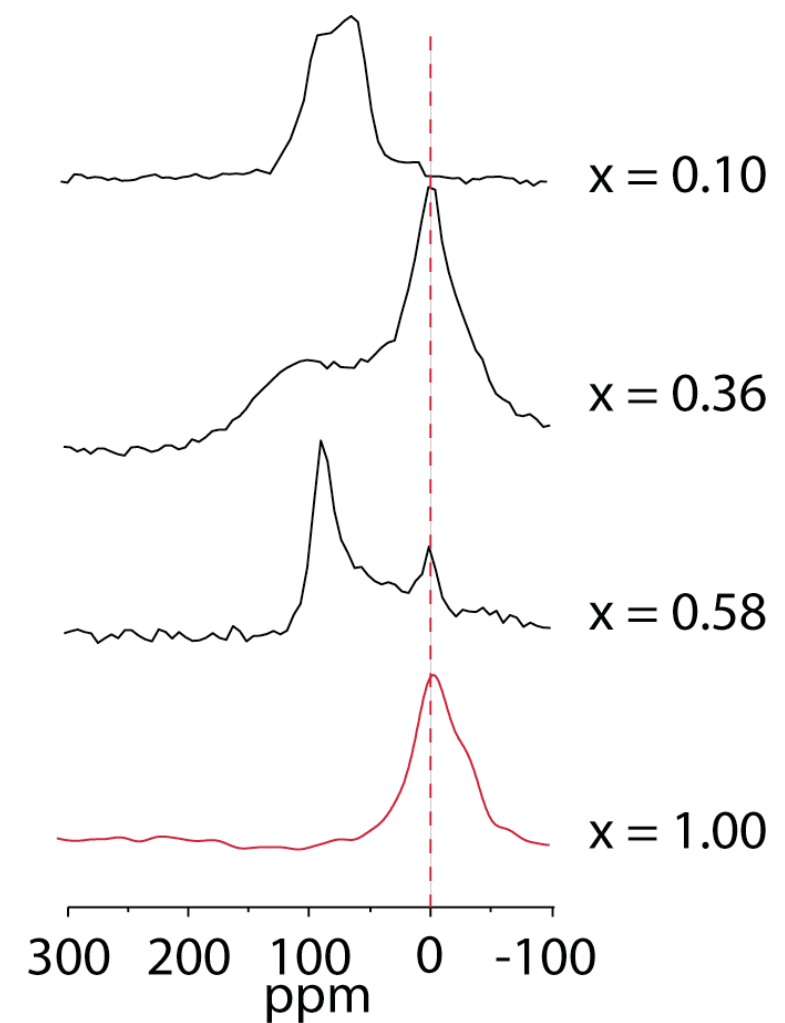
along c

LiNiN: MAS

- ★ $x < 1$: temperature-dependent paramagnetic shift consistent with Curie-Weiss paramagnetism
- ★ $x = 1$: small contact shift with negligible temperature variation consistent with band structure



lithium-6 MAS spectra at 20 kHz



referenced to LiCl(aq)

Summary (lithium metallonitrides)

Synthesis: ternary transition metal substituted nitrides $\text{Li}_{3-x-y}\text{M}_x\text{N}$ with controlled vacancy and substitution levels

Diffraction: lattice parameters a and c vary smoothly with x

Wideline lithium-7 NMR: E_a for intra-layer diffusion generally decreases with x , onset temperature of inter-layer diffusion raised with Ni, lowered with Cu

NMR Spin-lattice Relaxation: confirms the above

Computation: band structure of LiNiN suggests I-D metal

Lithium-6 MAS: consistent with computed band structures and magnetic susceptibility measurements

Summary

Lithium-6 and lithium-7 NMR allow much information to be obtained about lithium superionic conductors.

The low magnetogyric ratio and quadrupole moment for **lithium-6** result in better resolution of different local lithium environments, allowing studies of the role of **defects** in ionic conduction and changes in **structure** on extended cycling.

The broad quadrupolar lineshape observed for lithium-7 is more suitable for studies of dynamics and a **universal dynamical behavior** has been observed for a range of lithium superionic conductors using lineshape studies. Lithium-7 **exchange NMR** provides detailed information about timescales and mechanisms of diffusion.